energies

MDPI

Article

Optimized Operation and Sizing of Solar District Heating Networks with Small Daily Storage

Régis Delubac, Mohammad Sadr, Sabine Sochard, Sylvain Serra and Jean-Michel Reneaume *

LaTEP, E2S UPPA, Universite de Pau et des Pays de l'Adour, 64000 Pau, France
* Correspondence: jean-michel.reneaume@univ-pau.fr

Abstract: To continue improving the integration of solar thermal in district heating networks, optimization tools that can study both sizing and operation of heating plants are needed. In this article, the ISORC tool was used to study the sizing and coupled operation of smaller storage and solar fields with other heating sources such as biomass and gas boilers. For this, a k-medoids algorithm was applied to select consecutive characteristic days to size the system based on an optimal operation of consecutive days in the same season. The formulated problem was nonlinear, and the objective function to be minimized was the total cost. Two case studies with different day constructions and distributions were studied with various sensitivity analysis. The formulation and methodology allowed us to study different cases and situations easily and proved the importance of the selection and attribution of typical days. In all cases, the results showed that even with a daily approach, solar thermal covers approximately 20% of the demand, which demonstrates the relevance of considering and developing small daily storage with small solar fields.

Keywords: solar thermal energy; district heating networks; multi-sources; economic nonlinear optimization; typical days

Citation: Delubac, R.; Sadr, M.; Sochard, S.; Serra, S.; Reneaume, J.-M. Optimized Operation and Sizing of Solar District Heating Networks with Small Daily Storage. *Energies* **2023**, *16*, 1335. https://doi.org/10.3390/en16031335

Academic Editors: Mirko Morini and Costanza Saletti

Received: 6 December 2022
Revised: 18 January 2023
Accepted: 22 January 2023
Published: 27 January 2023

1. Introduction

District heating networks are viewed nowadays as a mature technology to decarbonize heating sources in cities and communities, which are one of the essential axes to limit global warming. Indeed, the residential-tertiary sector is responsible for 10% of the CO_2 emissions worldwide [1]. This decarbonization will be achieved through the integration of renewable heating sources such as solar thermal, geothermal or biomass power. Various project worldwide have demonstrated the relevance of using renewable sources to supply heat [2,3]. The challenge is to identify the optimal integration of these sources considering costs, CO_2 emissions, and efficiency.

Mathematical optimization has shown its relevance to the decarbonization of district heating networks (DHNs) by optimally integrating geothermal sources [4] or biomass sources [5,6] or by optimizing the distribution of heating and cooling [7,8]. The number of studies dealing with the optimization of DHNs has increased significantly over the last decade [9]. One of the reasons is that matching supply and demand in a district heating network is complex. Moreover, DHN systems are composed of several sub-elements, and the in-depth study of these elements over the total lifetime of the installation requires the use of adequate numerical tools. Numerous articles summarize existing optimization work [10–12], as numerical optimization has proven to be suitable for the study of DHNs due to its ability to study different complex scenarios over large time horizons. These papers [6,10,11] address both the optimization of the network structure, its sizing and its operation either with an overall view requiring many approximations or a more restricted view allowing the use of accurate models.

In the present paper, we focus on solar thermal integration in district heating networks using mathematical optimization.

2. State of the Art

2.1. Optimization of Solar District Heating Networks (SDHNs)

To study the integration of solar thermal energy in district heating networks, a dynamic approach is needed to consider the variability of solar availability and demand.

Here, two of the most commonly used approaches are presented. In the first approach, we deal with the dynamics of the system. We can use Pontryagin's principle (optimal control), which applies the optimality conditions to the Hamiltonian leading to a differential algebraic system to be solved with an appropriate integration method, such as Gear's method. Otherwise, we can formulate a constrained optimization problem with differential algebraic equations (DAE) as constraints. Then, discretization enables us to formulate the dynamic problem as an algebraic problem in order to use an appropriate algorithm depending on the formulated problem (non linear programming (NLP), mixed integer linear programming (MILP) or mixed integer non linear programming (MINLP)). Orthogonal collocation is a very efficient method to discretize differential equations, as it can be found in the articles of Powell et al. [13,14] that have proposed the dynamic optimization of a concentrated solar field as well as the sizing of a stratified two-volume thermocline storage. The authors also optimized the operation of a plant coupling solar thermal energy with a fossil fuel source, showing the significant share of recoverable solar and the existing synergies between these two sources. To optimize the sizing and operation of a low-temperature solar field with thermocline storage, Scolan et al. [15] optimized the solar power plant by minimizing the operating costs. One of the notable contributions was the addition of a tracker on the solar panels in order to follow the solar trajectory to improve the solar production or to deviate in order to protect the systems from excessive temperatures. In such dynamic approaches, the number of equations can increase significantly depending on the number of points used in the discretization scheme. Dynamic approaches are, therefore, often limited to studies with short time horizons if users wish to have a solution within reasonable computing times. Faced with this double observation, another dynamic approach needs to be proposed to solve problems over a long time horizon with short calculation time.

The multi-period approach takes position between the dynamic approach and quasi-static one, which represents the dynamic as a succession of steady state problems. To continue considering the dynamic of the system, a finite difference discretization of important differential terms of the model is set up, while the other terms are considered as steady states.

In [16], Powell et al. optimized the integration of storage in multi-energy networks by demonstrating the economic gains made by optimizing the use of storage. The study focused exclusively on operation with an MINLP approach to decide to operate some cooling sources or not. The authors proved that good storage operation could reduce costs by 16.5%. Haikarainen et al. [17] proposed an MILP model to optimize the structure and operation of a multi-energy network. One of the notable contributions was the use of pipelines that included both feed and return (to reduce heat losses), but the temperature levels were not considered, as in most of the linear approaches, which reduces the accuracy of renewable source integration. The calculations were performed via the Matlab interface and Cplex MILP solver in about 15 min. Fazlollahi et al. [18] also used the MILP approach to optimize the sizing and operation of multi-energy networks (heat and electricity), taking into account six types of technologies with a multi-objective optimization (costs and CO_2 emissions). Salame et al. [19] developed a multi-period MILP model that took into account conversion means such as heat pumps and organic Rankine cycles. Two types of periods (mini- and macro-periods) were defined, allowing independent management of the operation of the energy storage (integrated on micro-periods) and the investment (integrated on macro-periods). Different temperature levels were considered for the thermal integration of flows; however, the network itself was not modeled, which did not allow studying the evolution of flowrates or temperatures in the heating network. For NLP approaches, Tveit et al. [20] proposed an MINLP model optimizing the operation and structure of combined heat and

power (CHP) networks, taking into account long-term storage. Thirteen periods were used to represent 1 year, and the full time horizon was 6 years. The commercial solvers used were Cplex for the MILP part and CONOPT for NLP with GAMS interface.

Optimization of solar integration in networks was studied by Carpaneto et al. [21], who modeled a solar source integrated into the energy mix of a CHP network. The authors concluded that a good use of storage allows reaching 100% solar in summer and mid-seasons. Rehman et al. [22] compared the performance of centralized and decentralized single-source solar heat networks at the neighborhood scale. Although conducted under Nordic conditions, the study highlighted the relevance of the decentralized configuration for the studied cases. Finally, we mention the work of Buoro et al. [23], who performed the optimization of a cogeneration system accompanied by a solar heating network. The authors used an MILP formulation to optimize the operating, concession and maintenance costs of the entire energy supply. Therefore, the different energy sources were sized accordingly. The solar field supplied an industrial area in northern Italy. The paper showed that the optimal sizing of the solar field could provide 55–60% of the energy required by the consumers. Other optimization studies allowed promoting the use of solar energy, as Saloux and Candadeno [24] showed the interest in using optimization in order to improve the operation of storage coupled with solar thermal in Canada, and it allowed reducing fossil energy consumption up to 30%. With an application case in Chile, Maximov et al. [25] studied how solar thermal could replace low-quality biomass fuel, and optimization work resulted in a reduction of 90% of CO_2 emissions in exchange for an increase of 20% in the levelized cost of heat.

Finally, Delubac et al. [9] used a multi-period approach to optimize both the sizing and operation of a solar district heating network through an NLP approach. This work was part of the ISORC project, which aims to create a fast and accurate tool to integrate solar into district heating networks. Results demonstrated that for an application case in southern France (Mediterranean climate), by minimizing costs (operational and capital expenditures), a 49% solar coverage was obtained. The speed of the tool allowed conducting various other sensitivity studies, for example, of the impact of operating parameters on the renewable rate needed to guarantee the heat supply or the optimal storage connection to the production plant. The present article is a continuation of this previous work.

2.2. Existing Tools to Promote Renewable Energies in DHNs

The number of energy network analysis tools has steadily increased in recent years. Three areas are particularly studied, namely electricity networks, heating networks and transport networks. Many tools are designed to cover each of these three sectors. Some tools, such as TRNSYS [26], are made for accurate simulation and analysis, while others, such as energy plan [27], study systems at a larger scale. A review of existing tools was conducted by Conolly et al. [28] in 2010 and more recently by Limpens et al. [29]. In their article, Hörsch et al. [29] introduced the Python for Power System Analysis (PyPSA) tool that permits study of the production and transmission of electricity across all Europe, but thermal modeling is not robust yet. Limpens et al. [30,31] presented Energyscope TD, a powerful tool for the optimization of multi-energy networks on a variable scale (urban to national scale). The authors aimed at creating a free and open-source tool allowing one to create characteristic days of a year with an hourly time step (which makes it possible to consider inter-seasonal storage), and then to optimize the operation and sizing of such networks in short computation times on a standard computer. As in most of the tools surveyed [28,32–34], the approach used is the MILP approach, which limits the tool to a simplified consideration of energy production and cost modeling. Energyscope TD is very relevant on large scale systems such as countries. The authors analyzed the energy transition possibilities for Belgium up to 2035. However, when it comes to sizing and optimizing a network on a local scale, the tool lacks accuracy.

The energetic systems under study experience large variations in demand and renewable sources. Due to this variation, hourly data are usually employed for the calculation in

order to accurately optimize and analyze the system. Nonlinear approaches allow considering more precisely some phenomena such as size effects or specific operational constraints but consequently increase the problem's complexity. This huge data set leads to a heavy computational burden. To reduce the simulation/optimization horizon from the whole lifespan of study to a horizon that can be easily solved, typical days must be used.

2.3. Selection of Typical Days

Typical days (TDs) or characteristic days are seen as a relevant trade-off between the approximation error in the representation of the energy systems and computational times. Selecting typical days is an important issue, since it affects the numerical cost and precision of the calculation. There are various methods and approaches in the literature to select TDs. Using heuristic rules is the easiest way to fulfill this TD selection [35]. To design and optimize an energy system, heating, cooling, and electricity demands are usually considered. To estimate these demands, a study was carried out by Lozano et al. [36] for a period of 1 year distributed in 24 characteristic days, where each day is divided into 24 hourly periods. One working day and one weekend day were selected for each month. A cumulative energy demand (CED) graphic method was proposed by Ortiga et al. [37] to select the typical days and their occurrence to represent the energy demand of an entire year. In another study, from G. Mavrotas et al. [38], a typical day with an hourly basis per month was chosen using a heuristic approach. Besides their model for application of the minimax regret criterion, two additional cases were studied. The first one was compressed into six seasons with 12 intraday (6×12) periods, and the second one, smaller, represented three seasons with six intraday (3×6) periods. To perform this aggregation, a technique to identify and group the months and hours that have similar demands (heating, cooling, and/or electricity) was established. M. Casisi et al. [39] used three kinds of typical days for the winter, summer and middle seasons of thermal and electrical energy demand of six buildings. On the other hand, 24 kinds of typical days for electric energy sold to the grid were taken into account. Another approach commonly used in the literature is the clustering method presented by F. Domínguez-Muñoz et al. [40] to extract typical days for the heat and cold loads of a system. User intervention is required to determine the number of typical days in addition to the peak days for heating and cooling demand. Repetition of each typical day is determined with this method.

The different methods described here all have their own criteria to check how close the TDs are to the real data and how to improve their similarities. The clustering method is able to classify the data that are the most similar. A combined heuristic and clustering method is employed here to reduce the dimension of the optimization model to a manageable size.

2.4. Objectives of the Present Work

Many articles have proven the relevancy of seasonal storage to decrease costs and CO_2 emissions of SDHNs [41,42]. Instead of focusing on macro scale multi-energy networks, which requires many hypotheses to linearize and reduce computational times, this work focuses on the sizing and operation of a heating plant in a district heating network in order to allow better accuracy when modeling components.

This article studies whether daily storage coupled with solar is a relevant technology to reduce costs and increase renewables in DHNs. Indeed, because DHNs are especially relevant for dense urban areas, large storage and solar fields are not often considered. However, it is interesting to estimate how much solar coverage can be obtained by minimizing costs if a small-scale storage is considered. Through this paper, we aim to contribute to the use of solar thermal in district heating networks and to show its relevance combined with small thermal energy storage. For this, we continued optimizing the operation and sizing of an SDHN, but based it on the consecutive operation of multiple days by seasons. In this paper, we first present the ISORC tool model, followed by the strategy used to create relevant typical days to solve small thermal energy storage (TES) optimization problems.

This model is then applied with various typical day approaches to carry out different sensibility studies to promote solar power in DHNs.

3. Methodology

In this paper, we used the ISORC tool presented by Delubac et al. [9], which uses a non linear programming (NLP) model. It proved its relevance to sizing and operating SDHNs with seasonal storage. An adaptation of this methodology was performed to enable it to solve other kind of SDHNs, especially those with smaller storage that we qualified as daily storage.

3.1. The ISORC Tool

Figure 1 below shows the studied system, which was a production plant composed of a solar field and two boilers (biomass and gas) and a storage and demand side. Details on modeling of those components are presented in this part.

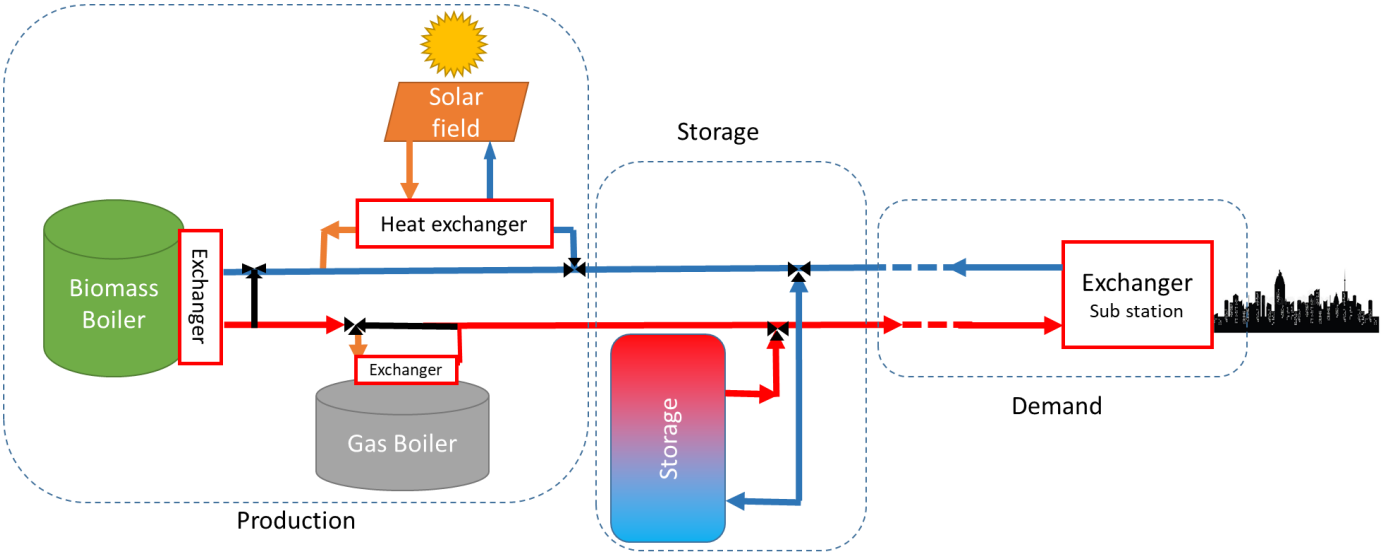

Figure 1. Presentation of ISORC tool configuration, which connects heating sources in series and the storage between the inlet and the outlet of the demand substation [9].

The ISORC tool was developed to optimize the sizing and operation of SDHN heat production sites. Consequently, the whole distribution network is modeled by a unique substation, which considers the sum of all consumer demand for each time step. Three heating sources are considered and provide a certain power at each time step i. Those sources are:

- A solar thermal plant modeled by a unique panel whose characteristics are representative of all of the panels. This model estimates generated power, taking solar irradiance and external temperature into account, through the following equation:

$$\dot{m}_{sol,i}\, C_p \left(T_{out,pan,i} - T_{in,pan,i}\right) = A_{pan}\left[\eta_0 G_i - \alpha_1 (T_{av,i} - T_{ext,i}) - \alpha_2 (T_{av,i} - T_{ext,i})^2\right] \quad (1)$$

  A_{pan} represents the total surface area of the panel, $\dot{m}_{sol,i}$ the flow rate for solar irradiance G_i, and coefficients η_0, α_1 and α_2 are dependent on the characteristics of the panel ($\eta_0 = 0.906$, $\alpha_1 = 3.36$ W/m^{2}K and $\alpha_2 = 0.0109$ W/m^{2}K^2, issued from the website "the solar keymark" [43]).
- One gas boiler and one biomass boiler, calculated as follows:

$$P_{boil,prod,i} = \dot{m}_{prod,boil,i} C_p \left(T_{out,boil,i} - T_{in,boil,i}\right) \quad (2)$$

$P_{boil,prod,i}$, is the boiler power supplied to the network. This power corresponds to the power of the boiler $P_{boil,i}$ multiplied by efficiency η_{boil} (Equation (3)) which depends on the boiler type (boil = biom "or" gas).

$$P_{boil,prod,i} = P_{boil,i}\,\eta_{boil,i} \tag{3}$$

This boiler power is also calculated as a ratio of the maximum power that the boiler can provide:

$$P_{boil,i} = K_{boil,i}\,P_{boil,max} \tag{4}$$

Moreover, the biomass boiler has additional constraints that do not allow the boiler to operate under a threshold value $K_{treshold}$, and the derivative of $P_{boil,i}$ is bounded [9].

The storage is modeled with two perfectly mixed (hot and cold) zones that vary in temperature and size over time but that cannot exchange heat with each other. The energy balance per zone results in a differential equation due to the presence of an accumulation term. The finite difference discretization of this differential term links together periods i and $i + 1$. Concerning the objective function, it consists in minimizing the total costs, summing of operational expenditures (OpEx), divided into P1 fuel consumption, P2 operation base maintenance, P3 annual maintenance, and capital expenditures (CapEx) as shown in Equation (5). Costs are based on references data supplied by the partners of the ISORC project, all specialists in DHNs, and solar thermal power plants.

$$\begin{aligned} Objective = \min(&CapEx_{sol} + \text{OpEx } P2_{sol} + \text{OpEx } P3_{sol} + CapEx_{stor} + \text{OpEx } P1_{biom} + \text{OpEx } P2_{biom} \\ &+\text{OpEx } P3_{biom} + CapEx_{biom} + \text{OpEx } P1_{gas} + \text{OpEx } P2_{gas} + \text{OpEx } P3_{gas} + CapEx_{gas}) \end{aligned} \tag{5}$$

This non-linear model is solved with a three-step resolution strategy [9] to first size an SDHN with simplified storage, then a storage alone, and both results will initialize a complete SDHN with the model presented above. This step-by-step resolution strategy is coupled with an initialization strategy that runs four parallel initializations:

- random initialization of all variables.
- random perturbation of the initializations of four sensitive variables, which are biomass maximal power, gas maximal power, surface area of solar field and storage maximal power;
- random perturbation of the bounds of those sensitive variables.
- random perturbation of both the bounds and initialization of those four variables.

3.2. Method to Create Typical Days

Here, some advanced methods are used to find TDs. The clustering method [40] is a technique to gather data that are the most similar in a group. Each group including a set of data is called a cluster. The member that is the most centrally located in the cluster is then chosen to represent the data of the cluster. Finally, the entire data set will be represented by a limited amount of data. The difficulty is to define the boundaries of these clusters. The data included in each cluster need to be as similar as possible. Partitional clustering is a method based on the optimization of an objective function. The "k-means" and "k-medoids" algorithms are the most popular. The k-means algorithm works by minimizing an objective function based on the Euclidean distance of the members of each cluster relative to their mean. Objects are then placed in clusters to minimize the sum of these distances in all of the clusters [37]. In this study, hourly data are accessible during a year. This set of data comprises power consumption [W] on the demand side, sun radiation [W], and temperature (°C), so D, the number of sets, is equal to 3. All of these data should be scaled in the computation and are normalized to the maximum values for each data type. The objective function of the k-means algorithm can be written as follows:

$$objective = \sum_{j=1}^{k} \sum_{x \epsilon c_j} dis\left(x, \mu_{C_j}\right) \tag{6}$$

In this equation, the initial data is denoted by x, a temporal series of elements known at every time step, μ_{C_j} represents the mean of cluster j or centers, and k is the number of clusters.

$$dis\left(x, \mu_{C_j}\right) = \sqrt{\sum_{d=1}^{D} \left(x_d - \mu_{C_d}\right)^2} \quad Euclidean\ distance \tag{7}$$

Euclidean distance is employed here as the criterion used in Equation (6). Since all parameters are independent, each one could affect the optimal point of the system. Thus, the resolution will search for the best trade-off between all of those parameters.

The k-medoids algorithm, which is an improvement of k-means, uses a function very similar to that of the k-means algorithm, except that instead of using the mean, data are used for the center of gravity and cluster representation. Thus, the k-medoids method uses the most central sample in the cluster as the representation of the cluster instead of receiving the mean values of the samples. To perform this modification, some procedures need to be added to the present algorithm. This allows the data closest to the mean value of the clusters to be chosen as new centers for the algorithm.

$$\mu_{C_j}{}' = Inf\left\{dis\left(x, \in_{C_j}\right), x \epsilon c_j\right\} \tag{8}$$

$\mu_{C_j}{}'$ is called centroid and represents the data belonging to cluster j that are closest to the mean μ_{C_j} according to the Euclidean distance. This point is selected as the new center for the next calculation in each cluster or group. So, Equation (6) is rewritten as follows:

$$Objective\ = \sum_{j=1}^{k} \sum_{x \in c_j} dis\left(x, \mu_{C_j}{}'\right) \tag{9}$$

Figure 2 below shows the steps to implement the k-medoid algorithm presented in [44]. It takes the number of clusters as the input parameter and the initial centers randomly determined. The distance of each data set to the centers is calculated. Each data set is assigned to the center with the closest distance. Then, the clusters are created. In the next step, centers are updated. In k-means, the new center is calculated by the average distance between all the data sets in each cluster; then, this new point is considered as the new center. However, in k-medoids, the closest data set to this average point is selected as shown in Equation (8). At the final step in Equation (10) where t represents the current iteration, it should be checked if the new center is equal to the center in the previous iteration or not. If equal, the loop is terminated, and the centers in the current iteration are determined as the selected data.

$$\mu_{C_j}{}^{t} = \mu_{C_j}{}^{t+1} \tag{10}$$

This method is implemented in Julia language programming to select TDs. The production is dependent on consumption, and it is a function of meteorological variables. That means these data are critical to find the optimal design and operational status of the system. Power consumption, irradiation and temperature are not equally important in reality and for the optimization model. This point is considered in the TD selection method by using priority coefficients. In Equation (11) the error load duration curve (ELDC) index is introduced. This index, commonly used in the literature [35,39,40], could be defined for each data profile, such as consumption power, sun irradiation, and temperature. This criterion, calculated retrospectively, makes it possible to characterize the representativeness of the selected TDs.

$$ELDC_j = \frac{\sum_{i=1}^{n} \left|\mu_{C_j}(i) - x(i)\right|}{\sum_{i=1}^{n} x(i)} \tag{11}$$

In this equation, n represents the total number of points in the considered time profile, $x(i)$ is the real data at time t, and $\mu_{C_j}(i)$ shows the representative or typical data selected in cluster j, at time i, for the current iteration.

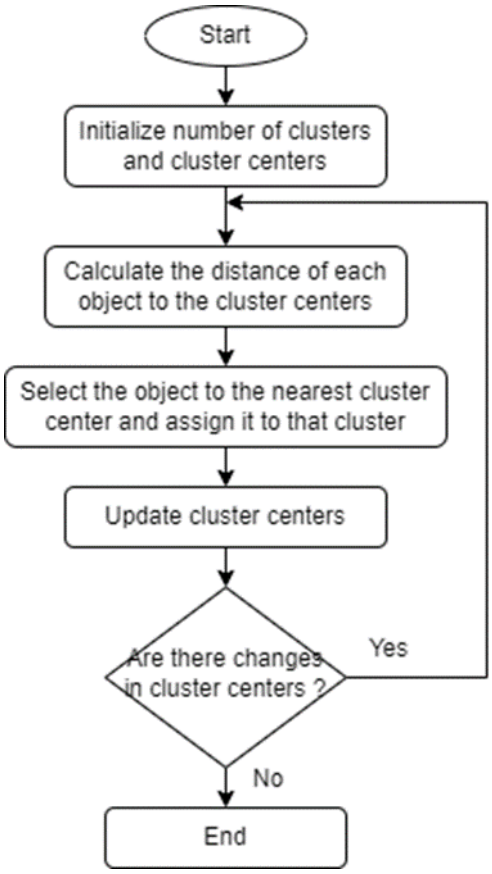

Figure 2. Strategy for resolution in the k-means algorithm.

3.3. Novelties of the ISORC Tool

In order to optimize the operation of characteristic days, seasons will be represented by two consecutive days with the same number of occurrences for summer, winter and mid-season. This consideration will permit us to observe how the operation of two different consecutive days is performed to reduce global costs. Consequently, the storage constraints are modified from yearly operational constraints to daily ones. Because the storage will be a daily constraint, storing heat during the summer to use it in the next seasons will not be allowed. Consequently, we have the following constraints with the index zone, which can take the value of hot or cold, and season indices that can take the value of summer, winter, or mid-season, as presented in (12) below.

$$V_{zone,season,0} = V_{zone,\ season,ends} \tag{12}$$

Moreover, extreme days for winter and summer will be considered in order to size a production plant able to supply demand in critical cases. In winter, the aim will be to satisfy the maximum heat demand with very low temperature and solar irradiation, while in summer it will be to supply low demand with high solar availability. The impact on total costs and sizing of those extreme days will be estimated.

3.4. Application Case

The model presented above is applied to a new district heating network located in southwestern France. Demand is based on an average year over 20 years of data. Meteorological data are from a solar radiation data website (SoDa) [45] for the same location of the demand profile with an average year based on 50 years of data. Therefore, consumer behavior on weekends or weekdays is not represented. Various sensitivity studies are performed on the optimization by changing the bounds or constraints of some

parameters. For example, in France, a gas boiler is usually sized by the peak demand to secure the supply in critical cases. Nevertheless, the gas boiler is then oversized and almost never operated at its optimal rate. An extra application case was studied by updating the gas price to study the impact of the gas crisis on the energy mix and overall costs.

4. Results

The results were obtained with the resolution strategy presented by Delubac et al. [9], which combined a step-by-step resolution from a simplified model to the full complete case and a random initialization strategy to select the best optimum among all optimal results. The problem was formulated in Julia language [46]; its optimization package JuMP [47] and the NLP problem were solved with the open solver Ipopt. The resolution strategy was applied to solve the problem over 400 times in about 2 h with a convergence rate of approximately 30%.

4.1. Case Study 1: Six Typical Days, Two for Each Season

In this first application case, a combined method was used to select the typical days between manual classification and the k-medoids algorithm. The data were manually classified on a seasonal basis with three considered seasons: summer, winter, and mid-season (which considered both spring and fall), and two typical days were selected for each season (k = 2), so the total was 6 days. The k-medoids algorithm presented in Figure 2 was applied for each seasonal data set to create representative days for each season. To consider critical designs for the system, the critical data, including minimum and maximum power consumption, had to be extracted from the data set. So, the final six seasonally based days plus two critical days were obtained by this method.

Corresponding power, temperature, and sun irradiation for each typical day were calculated. Figure 3 below illustrates the typical days selected by the method to support the optimization program. It can be observed that in the summer, the consumption profiles were all very close, including the critical one. This provided the possibility of reduction from 8 to 6 typical days, considering one day for summer and one critical day with maximum power consumption (usually in winter). Figure 3 illustrates the full daily consumption power profile per hour during the year (grey curves) and the results for the selected consumption power by selection of representative days (colored curses). It also shows the daily sun irradiation profile and the daily temperature profile per hour during the year for the same consumption power typical days. Moreover, Figure 3 allows us to note that the method chose representative profiles that covered the whole range of possibilities, which allowed expectations of a good estimation. The defined ELDC criterion was equal to 15.17% for this case. Compared to the case with 8 typical days having an ELDC equal to 14.67%, the assumption of considering 6 days allowed a reduction of computational effort and increased the chances of finding a solution.

The optimization was carried out to minimize total costs over a period of 20 years. For this first application case, we optimized the operation of three seasons represented by two characteristic days with an hourly time step that allowed us to solve a problem with 144 periods. The optimal sizing was 2493 m^2 of solar thermal, 116 m^3 of storage, 2640 kW of biomass and 4853 kW of gas, for a total cost of EUR 26.81 million. The hour-by-hour operation profile over the entire period was obtained, and we presented the operation obtained for each season. Indeed, the storage state of a characteristic profile must be the same at the end of a season as at its start, as expressed in Equation (12).

In winter, combined gas and biomass boilers are needed to satisfy the demand. On the first day, storage is even needed to meet peak demand and must, therefore, be discharged from the start. This discharge is followed by a charging phase on the following day to be at the same state as in the initial period. The biomass boiler is running at its maximal rate all along. Solar power allows for reducing gas consumption. Figure 4 shows that in winter, a larger solar field coupled with larger storage could permit even further reductions in gas

consumption. However, the solar share remains low either for economic reasons or since such a sizing could cause risks of overheating during the summer.

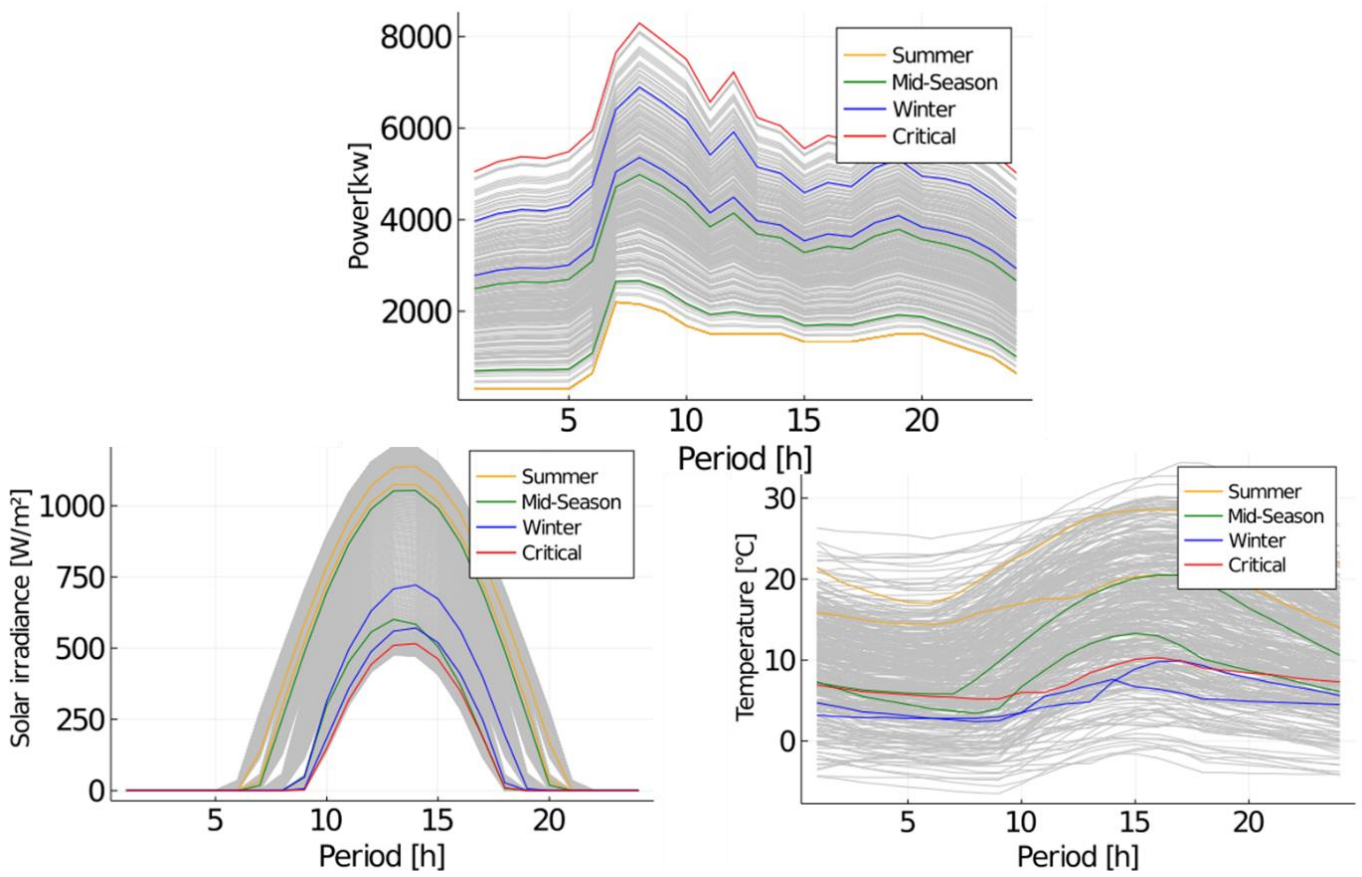

Figure 3. Representation of the selected days for case study 1 with colored lines among all profiles for power (thermal) demand, solar irradiance and external temperature.

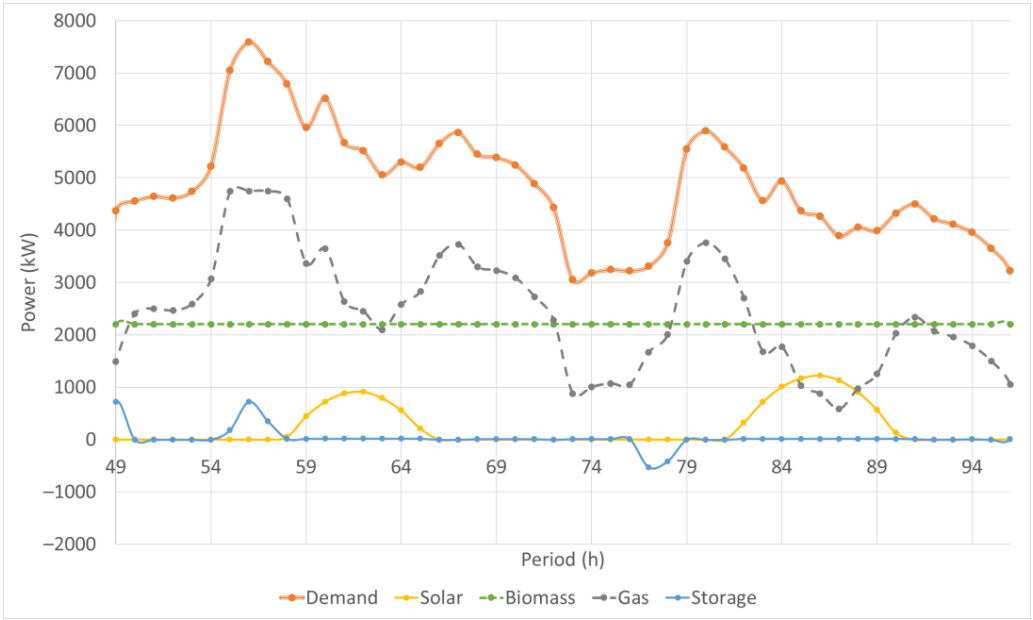

Figure 4. Optimal power operation for the first case study in winter (from time period 49 to 96) with representation of each source's operation profile.

For the mid-season represented in Figure 5, the gas boiler is operating to fulfill peak demand, coupled with storage which allows reductions in the power supplied by gas. The discharge of storage is fulfilled during one of the season's periods with lower demand and highest solar irradiance. In periods 120 and 124, storage is discharged because of the thermal inertia of the biomass boiler; indeed, to decrease the operation level from period 119 to 121, storage must be discharged in period 120 to adjust for the constraint in supply (production = demand).

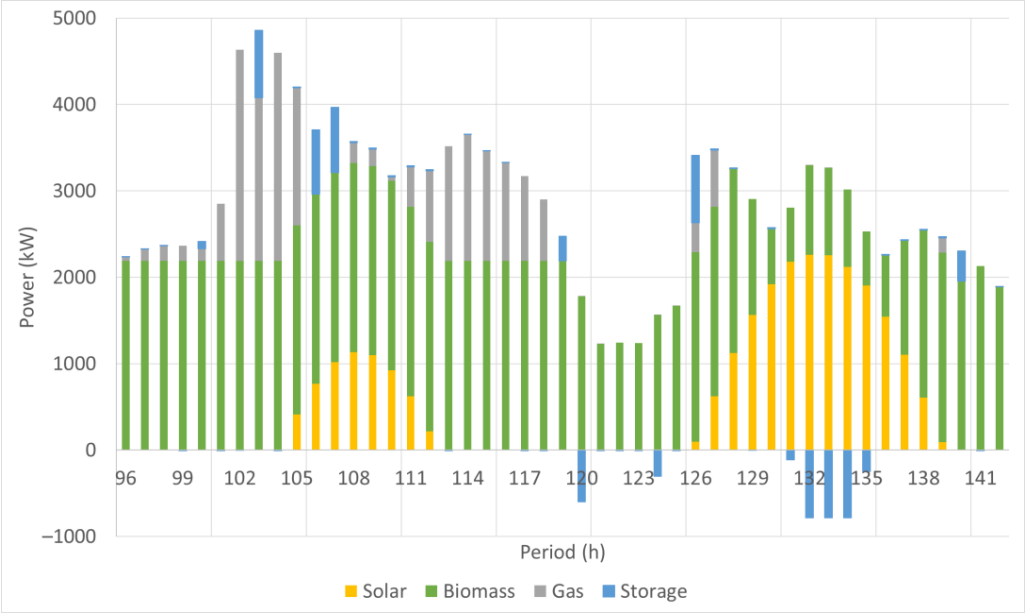

Figure 5. Optimal power operation/repartitioning for the first case study in mid-season (time period 96 to 144) with representation of cumulative power production.

Figure 6 shows the operations of all sources and storage implemented in order to supply the demand during summer. We observe that all long, the gas boiler is off; we can also see that the solar plant is sized to supply slightly more energy than the demand during summer (highest sunlight periods). The biomass boiler coupled with storage meets the demand when solar power is not available, with two noticeable operation modes: minimal operating rate on the first day or extinction on the second day. It can also be observed that storage must discharge during period 7 in order to fulfill the summer peak demand, since the biomass boiler is unable to achieve such production due to its inertia; the biomass boiler cannot go from the utilization rate in period 6 to one that meets maximal demand in period 7.

Figure 7 shows the energy mix for this case, which supplies the energy demand with a renewable rate of 72%. Solar power only represents 17% of the total mix, but this still shows the relevance of this technology in decarbonizing production. Moreover, during summer, solar covers 52% of the total demand, and storage permits the gas boiler to be idled during the whole season, which reduces the CO_2 emissions of the system (while the objective function is still to minimize costs).

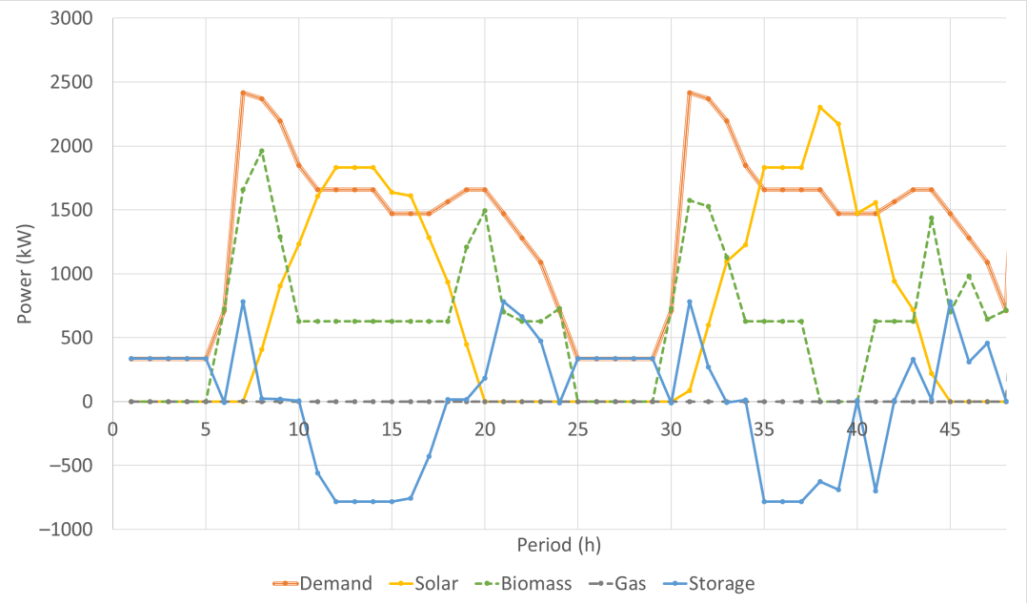

Figure 6. Optimal power operation for the first case study in summer (time periods 1 to 48), with representation of each source's operation profile.

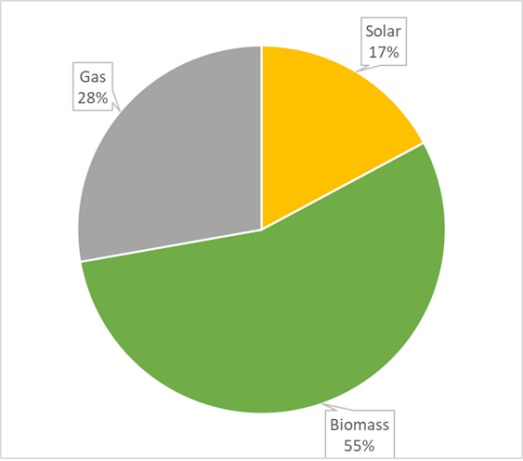

Figure 7. Energy mix of the first application case with six characteristic days.

It is interesting to compare Figure 7 with Figure 8, which shows the cost repartitioning of this optimal solution. We can observe that gas fulfills 28% of the demand and represents 33% of the total costs, while solar thermal supplies 17% of the demand with 11% of the costs. For this case, the investment and energy mix are closely linked.

4.1.1. Sensitivity Study: Gas Boiler Fixed as Constraint

One of the constraints usually added in France is to size the gas boiler in order to be able to supply the maximal demand alone. This constraint ensures the possibility of supplying heat even in the event of a breakdown of the biomass boiler, for example. Because the gas boiler is sized to meet the maximal demand, consequently, during winter, the period of highest demand, it is not required that storage be sized to be able to help meet the peak demand. Consequently, the operation of such a system is easier, but the total costs are about EUR 27.19 million, representing an increase of 1.4% (Table 1). In Figure 9, we observe that storage is not necessary to supply the maximal demand. Indeed, operation is easier: the biomass boiler is running at its maximal power, while solar power and the gas boiler

supply the additional heat. Concerning storage, the value is a little lower than zero for all periods, so there is a little charge all along, and a discharge in one period of the second day.

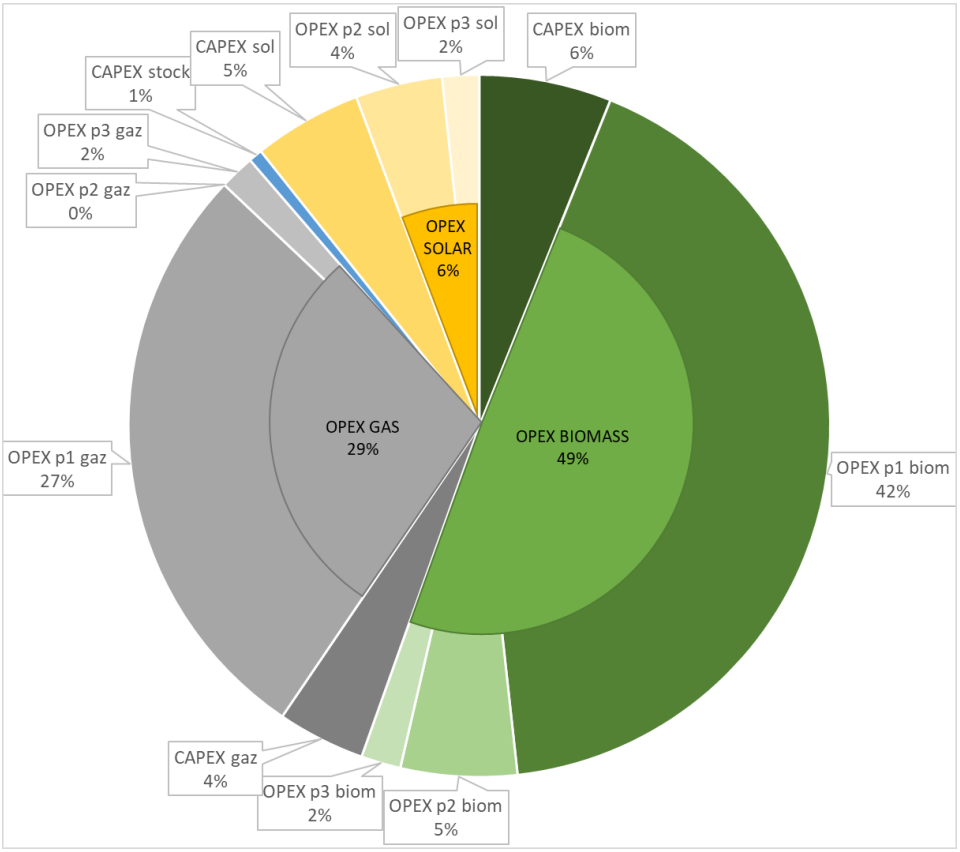

Figure 8. Cost repartitioning for the first application case with six characteristic days.

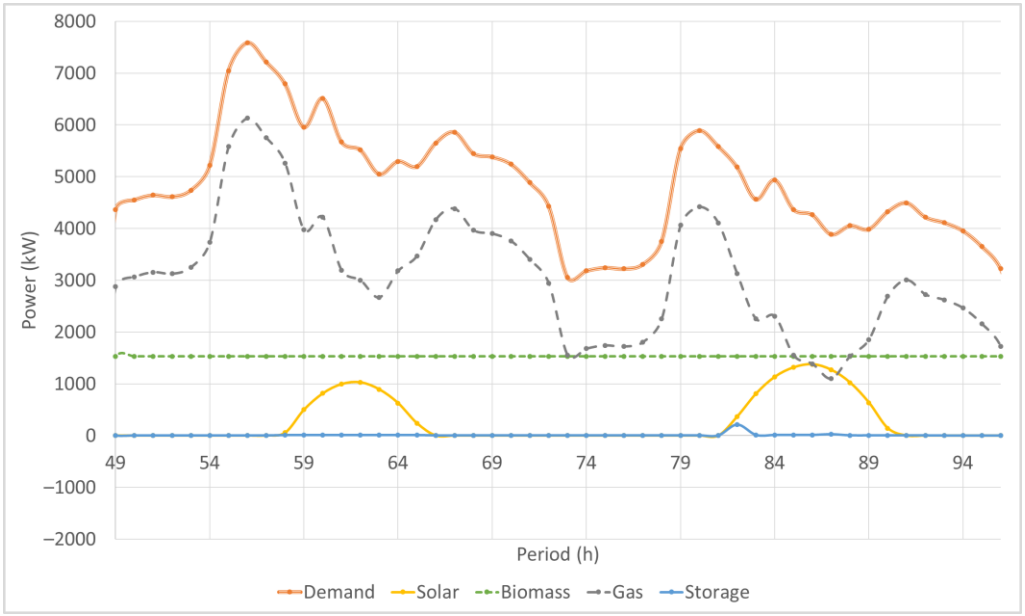

Figure 9. Optimal power operation for the first case study in winter (time periods 49 to 96), with representation of each source's operation profile.

Table 1. Sizing and costs for the first application case, comparing basic case, gas boiler maximized case, and critical day considered case.

Case	Solar Size (m^2)	Biomass Size (kW)	Gas Size (kW)	Storage Size (m^3)	Total Costs (Million EUR)	Renewable Rate (%)
Basic case	2493.18	2639.95	4852.84	116.32	26.81	72
Constrained gas boiler	2698.90	1842.17	6897.90	114.10	27.19	60
Critical day considered	3803.19	3223.53	8159.27	186.93	27.42	79
Actualization with gas crisis	2916.68	3588.23	4111.74	2227.31	29.01	85

4.1.2. Sensitivity Study: Consideration of Critical Days

A critical day is considered to size the heating plant in critical cases with low sun and/or high demand. They almost never impact the operational costs since a single day of operation can be neglected in comparison to the whole year. However, the sizing impact of this critical day can have an important influence on the costs, especially the CAPEX. If we consider the critical days (192 periods), the total costs are EUR 27.42 million (+2.28%). This is due to an increase in all production scales, from 52.3% for solar to 22.1% for the biomass boiler, as presented in Table 1, which compares the cases and results to observe the sizing and cost impacts of the hypothesis and sizing constraints. Figure 10 represents the operation of 3 × 2 characteristic days of operation followed by the critical day. We observe here that even with consideration for critical sizing, solar power remains a competitive source of heat. Most of the heat is provided by the biomass boiler, which operates at a constant rate during winter, and by the gas boiler, which supplies very low demand. This behavior is caused by the operational constraint (4), with the consequence that low demand cannot be supplied by the biomass boiler. On the critical day, all sources are used to supply the maximal demand, with storage charging with constant energy all day to discharge during peak demand.

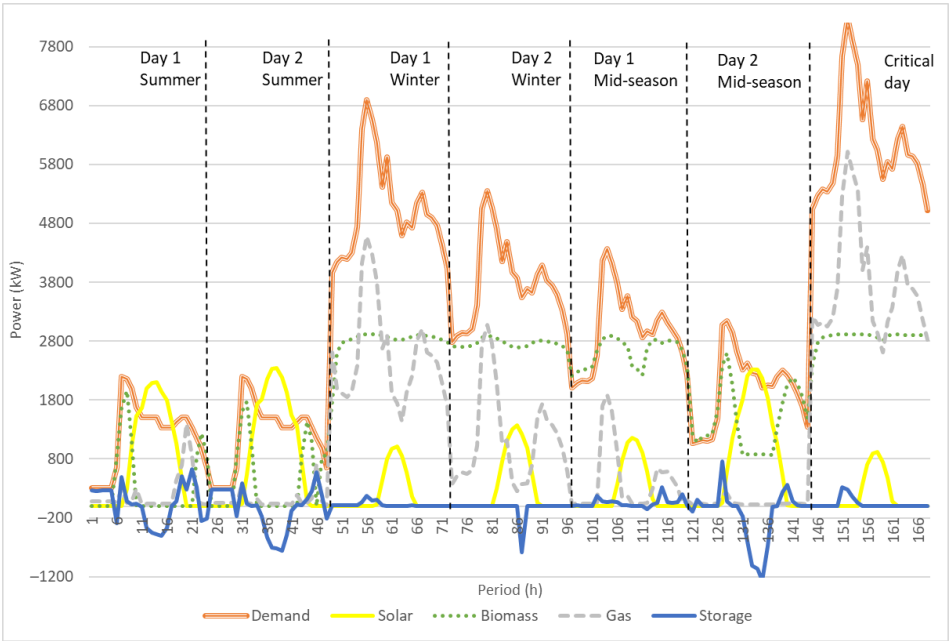

Figure 10. Optimal power operation of sources over the whole horizon, with consideration for critical winter day.

4.1.3. Sensitivity Study: Consideration of the Gas Crisis

An extra application case was established to consider the huge increase in gas prices (from EUR 0.04/kWh to 0.09/kWh) linked to the geopolitical situation of 2022. As a result, total prices, as expected, increased by 8.2% because gas is always needed to supply peak demand. However, the maximal size of the gas boiler decreased by 18%, to the benefit of the biomass boiler, which here covers 65% of the total demand (vs. 55% in the basic case), as shown in Figure 11.

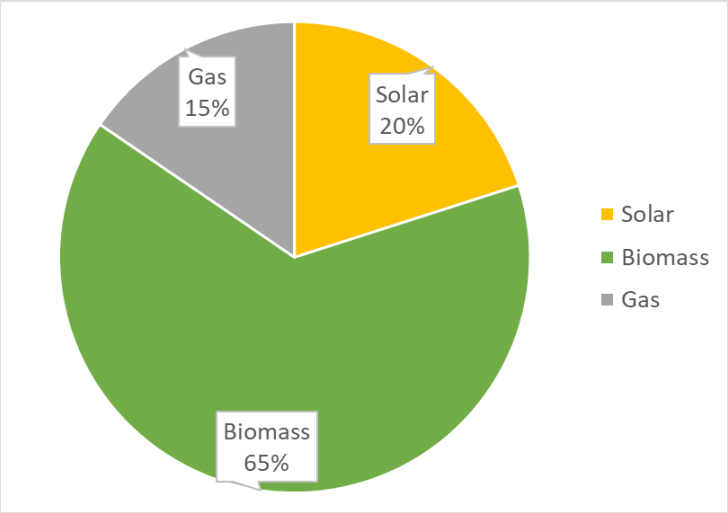

Figure 11. Energy mix for the first application case, considering the gas crisis and new costs.

Table 1 summarizes the different results for this first application case. The three cases studied during the sensitivity analysis (1—gas boiler designed to meet the maximum demand, 2—taking into account the critical day, 3—the increase in the price of gas due to the international crisis) obviously lead to a degradation of the objective function (cost increase), compared to the basic case. Detailed explanations of the evolution of the energy mix were presented in the previous paragraphs. However, the renewable rate changed substantially through the different studies. For example, the gas crisis linked to the war in Ukraine increased prices, but this is leading to a new energy mix with a higher renewable rate.

4.2. Case Study 2: Seven Typical Days, Not Considering Critical Day

In this second case study, typical days were extracted considering the following clusters. We consider here two winter days, three mid-season days, and one summer day (Figure 12). This choice is due to the fact that during summer, demand is very low regardless of the weather or temperature. Consequently, a single day can be a good choice to represent the whole season. Conversely, mid-seasons have more variable demand, which can change from one day to another; thus, studying one extra day of mid-season could be of interest. From the power consumption profile, it was concluded that typical selection days provide a reasonable estimation, although the critical typical day was not considered in this case. In this case study, the ELDC decreased from a value of 14.67% to 11.89%, which provided a more exact estimation compared to the previous case. This will affect the optimization results for the system.

As a result of this study, total costs were EUR 28.38 million, for an increase of 5%. We observed increases in all dimensions: of 1960 kW for biomass (+20%), of 214 m^3 in storage (+46%), of 5723.7 kW for gas (+15%), and of 4193 m^2 in area for solar (+68%), for a total renewable rate of 62%, 24% of which was for solar. Optimal operations on the three consecutive mid-season days are presented in Figure 13. Solar field and storage size, which were higher than in the preceding cases, allowed storing heat during the second day with the lowest demand profile. This stored heat permitted reducing the use of gas on the

preceding and next days. It highlights an operation where storage is first discharging, able able to charge later, and then to discharge again for high heat demand days. The biomass boiler is always operating between its maximal rate, which affords the best efficiency, and its lowest allowed operating rate. Both storage and gas are added to biomass heat to satisfy demand depending on the storage availability, as we see in period 79 when storage is charged with gas surplus heat, to be discharged in period 84 with the gas boiler shut down.

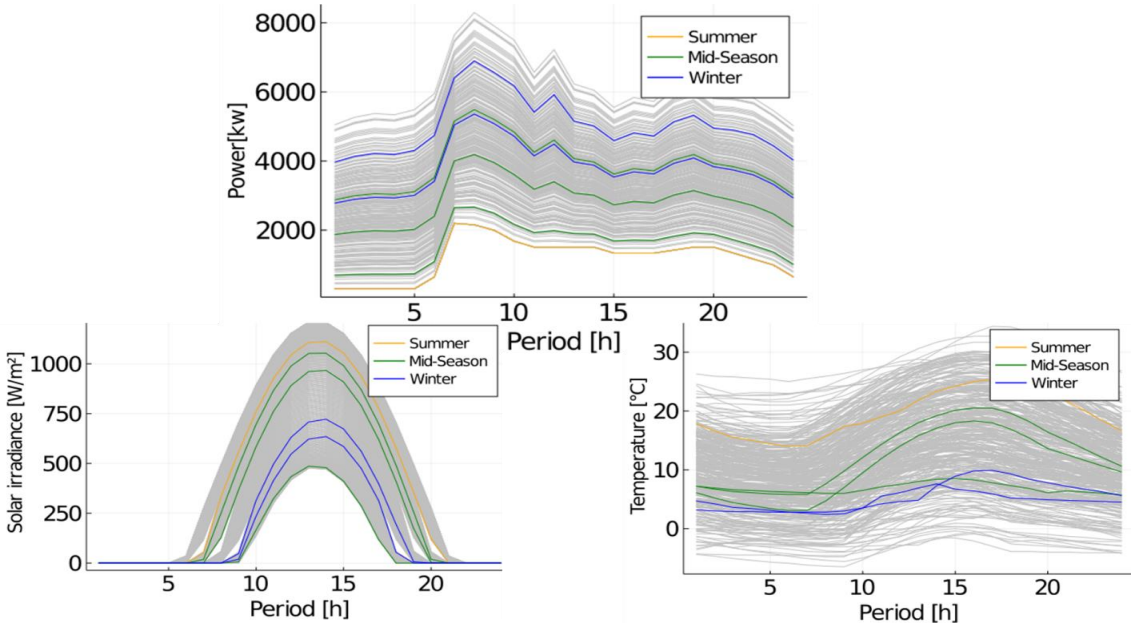

Figure 12. Representation of the selected days for case study 2 with colored lines among all profiles for power (thermal) demand, solar irradiance, and external temperature.

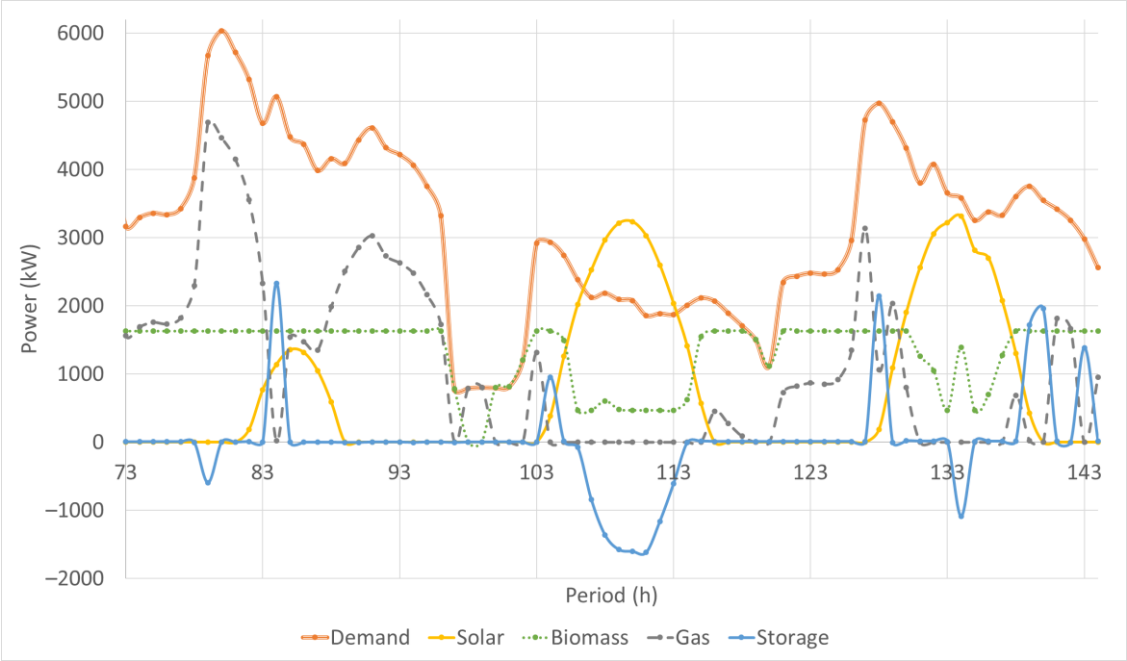

Figure 13. Optimal power operation for the second case study in mid-season (time periods 73 to 144), with representation of each source's operation profile.

These results based on identical input data show the importance of using characteristic days adapted to the study and the approach. Reducing the ELDC error resulted in a 5% difference in total cost.

5. Conclusions

In order to improve general knowledge amid the trend towards carbon neutrality, this contribution proposed a methodology for the optimization of the design and operation of heating networks including daily storage and small solar fields. We proposed the formulation of a multi-period nonlinear optimization problem. Particular attention was paid to the definition of the characteristic days, which is of particular importance considering the compromise between precision and the calculation load. ISORC, a robust software tool, has been developed to meet the needs of decision-makers: combining speed and precision, it allows the comparison of optimal solutions in different contexts, according to different hypotheses.

Two cases were studied with a different repartitioning of typical days selected to observe the optimal sizing and operation of storage to minimize costs. Results show that solar thermal always has value to be integrated in DHNs to supply heat even if the energy component is low. It is economically optimal to integrate such a technology even for places where the scales for storage and the solar field are limited.

The first application case for three seasons represented by two characteristic days with an hourly time step (144 periods) resulted in a total renewable rate of 72%, with 17% for solar power. Sensitivity analysis of various parameters such as sizing constraints, consideration for critical days, or gas price variations presented some sizing and operational particularities that were analyzed season by season.

The second application shows the importance of the choice of typical days. Since the supply of heat in the summer is less challenging, three typical days were used in mid-season and one less in summer. With these new parameters, the optimization resulted in a renewable rate of 62%, with 24% for solar power, and an energy mix similar in both cases.

In future works, it seems important to develop a methodology to define the number of characteristic days (and the profiles of these days) resulting from a compromise between accuracy and computation time. It is possible, for example, to be inspired by what has been done in computational fluid dynamics (CFD) to converge towards a stabilized mesh: gradually increase the number of characteristic days until optimal stabilized solutions are obtained (with respect to a tolerance given a priori).

Author Contributions: Conceptualization, R.D., M.S., S.S. (Sylvain Serra), S.S. (Sabine Sochard) and J.-M.R.; Data curation, R.D. and M.S.; Formal analysis, R.D., M.S. and S.S. (Sabine Sochard); Funding acquisition, S.S. (Sylvain Serra); Methodology, R.D., S.S. (Sylvain Serra) and S.S. (Sabine Sochard); Project administration, S.S. (Sabine Sochard); Software, R.D. and M.S.; Supervision, J.-M.R.; Validation, R.D., S.S. (Sylvain Serra), S.S. (Sabine Sochard) and J.-M.R.; Writing—original draft, R.D.; Writing—review and editing, S.S. (Sylvain Serra), S.S. (Sabine Sochard) and J.-M.R. All authors have read and agreed to the published version of the manuscript.

Funding: This research was funded by ADEME grant number 1805C0007 and the "Region Nouvelle-Aquitaine".

Data Availability Statement: Not applicable.

Acknowledgments: The authors would like to thank ADEME via the "Appel à projet de recherche ENERGIE DURABLE" and the "Region Nouvelle-Aquitaine" for providing funding for the ISORC/OPTIMISER project. The authors also thank their partners (Tecsol, NewHEAT and Sermet) for their valuable advice.

Conflicts of Interest: The authors declare no conflict of interest.

Nomenclature

A	area, m^2
C_p	specific heat, J kg^{-1} K^{-1}
D	number of sets for TD
G	global irradiance, W m^{-2}
K	utilization rate of boiler
k	number of clusters/data
$\dot{m}$	mass flow rate, kg s^{-1}
P	power, W
T	temperature, °C
V	volume, m^3
x	data of the series
Greek symbols	
α_1	first panel coefficient, W m^{-2} K^{-1}
α_2	second panel coefficient, Wm^{-2} K^{-2}
η_0	optical yield
η	efficiency
μ_{C_j}	mean of cluster j
$\mu_{C_j}{}'$	centroid of cluster j
Subscripts and superscripts	
av	average
biom	biomass boiler
boil	boiler
d	time step for TD selection
dis	distance
ext	external
i	time step
inf	inferior value
j	cluster index
in/out	inlet/outlet
min/max	minimum/maximum
pan	panel
prod	production
P1	operational cost of fuel
P2	operational costs of low maintenance
P3	operational costs of major maintenance
sol	solar
stor	storage
t	iteration of TD selection
Abbreviations	
CapEx	Capital Expenditure
CHP	Combined Heat and Power
DAE	Differential Algebraic Equation
DHN(s)	District Heating Network(s)
ELDC	Error Load Duration Curve
HEX	Heat Exchanger
	HHV
MILP	Mixed Integer Linear Programming
MINLP	Mixed Integer Non Linear Programming
NLP	Non Linear Programming
ORC	Organic Rankine Cycle
OpEx	Operational Expenditure
SDHN(s)	Solar District Heating Network(s)
Seas	Season
Sig	Sigmoid Function
TD(s)	Typical Day(s)
TES	Thermal Energy Storage

References

1. Ministère de la Transition Écologique. Chiffres Clés de L'énergie-Édition 2020. December 2020; p. 80. Available online: https://www.statistiques.developpement-durable.gouv.fr/sites/default/files/2020-11/datalab_70_chiffres_cles_energie_edition_2020_septembre2020_1.pdf (accessed on 15 October 2022).
2. Euroheat & Power. 2021. Available online: https://www.euroheat.org/knowledge-hub/resource-library-search.html (accessed on 15 October 2022).
3. Solar District Heating. 2021. Available online: https://www.solar-district-heating.eu/en/plant-database/ (accessed on 15 October 2022).
4. Marty, F.; Serra, S.; Sochard, S.; Reneaume, J.-M. Simultaneous optimization of the district heating network topology and the Organic Rankine Cycle sizing of a geothermal plant. *Energy* **2018**, *159*, 1060–1074. [CrossRef]
5. Noussan, M.; Abdin, G.C.; Poggio, A.; Roberto, R. Biomass-fired CHP and heat storage system simulations in existing district heating systems. *Appl. Therm. Eng.* **2014**, *71*, 729–735. [CrossRef]
6. Rezaei, M.; Sameti, M.; Nasiri, F. Biomass-fuelled combined heat and power: Integration in district heating and thermal-energy storage. *Clean Energy* **2021**, *5*, 44–56. [CrossRef]
7. Mertz, T.; Serra, S.; Henon, A.; Reneaume, J.-M. A MINLP optimization of the configuration and the design of a district heating network: Academic study cases. *Energy* **2016**, *117*, 450–464. [CrossRef]
8. Vesterlund, M.; Toffolo, A.; Dahl, J. Optimization of multi-source complex district heating network, a case study. *Energy* **2017**, *126*, 53–63. [CrossRef]
9. Delubac, R.; Serra, S.; Sochard, S.; Reneaume, J.-M. A Dynamic Optimization Tool to Size and Operate Solar Thermal District Heating Networks Production Plants. *Energies* **2021**, *14*, 8003. [CrossRef]
10. Sameti, M.; Haghighat, F. Optimization approaches in district heating and cooling thermal network. *Energy Build.* **2017**, *140*, 121–130. [CrossRef]
11. Gao, L.; Hwang, Y.; Cao, T. An overview of optimization technologies applied in combined cooling, heating and power systems. *Renew. Sustain. Energy Rev.* **2019**, *114*, 109344. [CrossRef]
12. Lake, A.; Rezaie, B.; Beyerlein, S. Review of district heating and cooling systems for a sustainable future. *Renew. Sustain. Energy Rev.* **2017**, *67*, 417–425. [CrossRef]
13. Powell, K.M.; Edgar, T.F. Modeling and control of a solar thermal power plant with thermal energy storage. *Chem. Eng. Sci.* **2012**, *71*, 138–145. [CrossRef]
14. Powell, K.M.; Hedengren, J.D.; Edgar, T.F. Dynamic optimization of a hybrid solar thermal and fossil fuel system. *Sol. Energy* **2014**, *108*, 210–218. [CrossRef]
15. Scolan, S. Dynamic optimization of the operation of a solar thermal plant. *Sol. Energy* **2020**, *198*, 643–657. [CrossRef]
16. Powell, K.M.; Kim, J.S.; Cole, W.J.; Kapoor, K.; Mojica, J.L.; Hedengren, J.D.; Edgar, T.F. Thermal energy storage to minimize cost and improve efficiency of a polygeneration district energy system in a real-time electricity market. *Energy* **2016**, *113*, 52–63. [CrossRef]
17. Haikarainen, C.; Pettersson, F.; Saxén, H. A model for structural and operational optimization of distributed energy systems. *Appl. Therm. Eng.* **2014**, *70*, 211–218. [CrossRef]
18. Fazlollahi, S.; Mandel, P.; Becker, G.; Maréchal, F. Methods for multi-objective investment and operating optimization of complex energy systems. *Energy* **2012**, *45*, 12–22. [CrossRef]
19. Salame, S. *Méthodologie de Conception de L'architecture D'intégration Énergétique des Procédés Variables Incluant des Stockages Thermiques et des Systèmes de Conversion D'énergie*; Mines Paris Tech: Paris, France, 2017; Available online: https://theses.hal.science/tel-01449262/ (accessed on 5 September 2022).
20. Tveit, T.-M.; Savola, T.; Gebremedhin, A.; Fogelholm, C.-J. Multi-period MINLP model for optimising operation and structural changes to CHP plants in district heating networks with long-term thermal storage. *Energy Convers. Manag.* **2009**, *50*, 639–647. [CrossRef]
21. Carpaneto, E.; Lazzeroni, P.; Repetto, M. Optimal integration of solar energy in a district heating network. *Renew. Energy* **2015**, *75*, 714–721. [CrossRef]
22. Rehman, H.; Hirvonen, J.; Sirén, K. Performance comparison between optimized design of a centralized and semi-decentralized community size solar district heating system. *Appl. Energy* **2018**, *229*, 1072–1094. [CrossRef]
23. Buoro, D.; Pinamonti, P.; Reini, M. Optimization of a Distributed Cogeneration System with solar district heating. *Appl. Energy* **2014**, *124*, 298–308. [CrossRef]
24. Saloux, E.; Candanedo, J.A. Sizing and control optimization of thermal energy storage in a solar district heating system. *Energy Rep.* **2021**, *7*, 389–400. [CrossRef]
25. Maximov, S.A.; Mehmood, S.; Friedrich, D. Multi-objective optimisation of a solar district heating network with seasonal storage for conditions in cities of southern Chile. *Sustain. Cities Soc.* **2021**, *73*, 103087. [CrossRef]
26. TRNSYS. Available online: http://www.trnsys.com/index.html (accessed on 4 December 2019).
27. Stergaard, P.A. Reviewing EnergyPLAN simulations and performance indicator applications in EnergyPLAN simulations. *Appl. Energy* **2015**, *154*, 921–933. [CrossRef]
28. Connolly, D.; Lund, H.; Mathiesen, B.; Leahy, M. A review of computer tools for analysing the integration of renewable energy into various energy systems. *Appl. Energy* **2010**, *87*, 1059–1082. [CrossRef]

29. Hörsch, J.; Hofmann, F.; Schlachtberger, D.; Brown, T. PyPSA-Eur: An open optimisation model of the European transmission system. *Energy Strategy Rev.* **2018**, *22*, 207–215. [CrossRef]
30. Limpens, G.; Moret, S.; Jeanmart, H.; Maréchal, F. EnergyScope TD: A novel open-source model for regional energy systems. *Appl. Energy* **2019**, *255*, 113729. [CrossRef]
31. Limpens, G.; Jeanmart, H.; Maréchal, F. Belgian Energy Transition: What Are the Options? *Energies* **2020**, *13*, 261. [CrossRef]
32. Wiese, F.; Bramstoft, R.; Koduvere, H.; Alonso, A.P.; Balyk, O.; Kirkerud, J.G.; Tveten, G.; Bolkesjø, T.F.; Münster, M.; Ravn, H. Balmorel open source energy system model. *Energy Strat. Rev.* **2018**, *20*, 26–34. [CrossRef]
33. Openmod-Open Energy Modelling Initiative. Available online: https://www.openmod-initiative.org/ (accessed on 4 December 2019).
34. Groissböck, M. Are open source energy system optimization tools mature enough for serious use? *Renew Sustain Energy Rev.* **2019**, *102*, 234–248. [CrossRef]
35. Limpens, G. *Generating Energy Transition Pathways: Application to Belgium*; Louvain School of Engineering: Ottignies-Louvain-la-Neuve, Belgium, 2021.
36. Lozano, M.A.; Ramos, J.C.; Carvalho, M.; Serra, L.M. Structure optimization of energy supply systems in tertiary sector buildings. *Energy Build.* **2009**, *41*, 1063–1075. [CrossRef]
37. Ortiga, J.; Bruno, J.C.; Coronas, A. Selection of typical days for the characterisation of energy demand in cogeneration and tri-generation optimisation models for buildings. *Energy Convers. Manag.* **2011**, *52*, 1934–1942. [CrossRef]
38. Mavrotas, G.; Diakoulaki, D.; Florios, K.; Georgiou, P. A mathematical programming framework for energy planning in services' sector buildings under uncertainty in load demand: The case of a hospital in Athens. *Energy Policy* **2008**, *36*, 2415–2429. [CrossRef]
39. Casisi, M.; Pinamonti, P.; Reini, M. Optimal lay-out and operation of combined heat & power (CHP) distributed generation systems. *Energy* **2009**, *34*, 2175–2183. [CrossRef]
40. Domínguez-Muñoz, F.; Cejudo-López, J.M.; Carrillo-Andrés, A.; Gallardo-Salazar, M. Selection of typical demand days for CHP optimization. *Energy Build.* **2011**, *43*, 3036–3043. [CrossRef]
41. Dahash, A.; Ochs, F.; Janetti, M.B.; Streicher, W. Advances in seasonal thermal energy storage for solar district heating applications: A critical review on large-scale hot-water tank and pit thermal energy storage systems. *Appl. Energy* **2019**, *239*, 296–315. [CrossRef]
42. Mangold, M.; Österbring, M.; Wallbaum, H. Handling data uncertainties when using Swedish energy performance certificate data to describe energy usage in the building stock. *Energy Build.* **2015**, *102*, 328–336. [CrossRef]
43. The Solar Keymark. 2021. Available online: http://www.solarkeymark.nl/DBF/ (accessed on 5 December 2022).
44. Deepali Arora, P.; Varshney, S. Analysis of K-Means and K-Medoids Algorithm for Big Data. *Procedia Comput. Sci.* **2016**, *78*, 507–512. [CrossRef]
45. Solar Radiation Datas Homepage. 2022. Available online: https://www.soda-pro.com/web-services#meteo-data (accessed on 8 December 2021).
46. Bezanson, J.; Karpinski, S.; Shah, V.; Edelman, A. The Julia Language. Available online: https://julialang.org/ (accessed on 4 December 2019).
47. Dunning, J.H.I.; Huchette, J.; Lubin, M. JuMP: A Modeling Language for Mathematical Optimization. *SIAM Rev.* **2017**, *59*, 295–320. [CrossRef]